Multi-Hop Range Extension of a Wireless Remote Control for Underwater Vehicles

Alberto Signori, Filippo Campagnaro, Michele Zorzi

Department of Information Engineering, University of Padova, via Gradenigo 6/B, 35131 Padova, Italy
{signoria,campagn1,zorzi}@dei.unipd.it

Abstract—In this paper, we explore the feasibility of controlling an Underwater Autonomous Vehicle (AUV) from a base station, via a multi-hop wireless control channel. As a first step, we identify which networking and data-link protocols can be employed in this system. Then, we design a simple but effective routing protocol for this scenario. Finally, we simulate the performance of the system during missions of interest, and conclude by discussing the effectiveness of wireless multi-hop control methods for AUVs.

Index Terms—Underwater acoustic communications; multi-hop underwater networks; AUV; simulation; DESERT Underwater

I. INTRODUCTION AND RELATED WORK

In the last years, underwater networks have been gaining more and more interest in both scientific and industrial areas. Traditionally, underwater networks have focused on surveillance and environmental monitoring tasks [1], not only for disaster prevention, but also to analyze water characteristics (such as salinity and temperature), monitor marine life, or observe geological processes on the ocean floor [2]. Underwater networks are also employed in the oil field, in order to monitor underwater pipelines and equipment for oil extraction [3]. In this specific scenario, thanks to the increasing capabilities of Underwater Unmanned Vehicles (UUVs) [4] and the recent development of non-acoustic underwater communication systems [5], [6], a heterogeneous and multimodal wireless network composed by both fixed nodes and underwater vehicles can be employed to operate in such a challenging environment. Such nodes and vehicles communicate with each other by employing either acoustic, optical, or electro-magnetic communications [7], so combining the advantages of each technology. While underwater acoustic modems provide a low rate and long range data link up to a few kilometers, both optical and electro-magnetic modems are employed for broadband short range communication, up to few tens of meters [8]. Underwater drones can be divided in two categories, namely Remotely Operated Vehicles (ROVs) and Underwater Autonomous Vehicles (AUVs). The former are usually tethered to a ship with a cable called umbilical, that supplies both data and power connections, and are driven in real time [4]. The latter, instead, are not tethered, and therefore cannot be controlled in real time in a long range scenario, as only acoustic communication can be used to exchange data between them and a remote base station. Two different position planning systems can be used to drive an AUV. In the first approach, a pre-chosen path is

uploaded to the vehicle at the beginning of a mission [9] and no interaction with a control station is required throughout the mission. This is the most commonly used strategy, where only the position might be monitored with either an ultra-short baseline (USBL) or a long baseline (LBL) acoustic positioning system [10], [11], without the need to establish a communication link. In the second approach, the AUV is driven by a remote control station that sends packets containing the coordinates of the way-points to which the AUV should head. Such approach is mostly employed in hybrid vehicles that operate like ROVs [12] and is often used when the original mission changes. In [7] the authors analyzed the feasibility of the control of an ROV in a single hop wireless network with focus on a short range scenario, where both optical and acoustic communication can be combined to achieve high throughput. In our paper, this analysis will be extended to a multi-hop acoustic network, in order to expand the range in which the vehicle can move and still receive commands sent by the control station (CTR). The drawback is an increase of the control latency, because the number of transmissions needed to forward a packet increases compared to the single hop scenario. Therefore, in this case the vehicle is considered to perform an AUV mission, as the resulting Quality of Services (QoS) of the remote control supported in such scenario is more relaxed with respect to the single hop case (e.g., neither video nor image transfer is supported), for the benefit of a wider coverage range.

In this paper we analyze the feasibility of the remote control of an AUV in a network with linear topology, composed by a fixed controller, N_{relays} fixed relays and a mobile node (AUV). Since in our scenario the distance between two nodes is in the order of kilometers, only long range acoustic modems can be employed for communication, as both optical and electromagnetic technologies are out of their coverage range. In Section II we describe the application employed to control the trajectory of the AUV and the acknowledgment (ACK) policy used for packet retransmissions. We consider a scenario in which the AUV can move anywhere along the network, as long as it remains in the transmission range of at least one of the fixed nodes, i.e., the relays or the control station. In such a topology, two main problems arise. The first problem is the need for a routing protocol to allow the communication between the AUV and the control station. In this scenario, static routing cannot be used because the AUV can be in any point of the network. In Section III we present two possible

routing protocols that can be employed in such a network. The second problem is how to design a proper Medium Access Control (MAC) layer to contrast the performance degradation due to the use of relays to deliver a packet, thus, in Section IV, we describe a MAC protocol that aims to mitigate this problem. In this scenario, described in Section V, we evaluate both the accuracy of the AUV position control and the amount of information the AUV can send back to the control station, e.g., monitoring data. In Section V, we also present the details of the simulation employed to evaluate this system, while the performance evaluation results are reported in Section VI together with a power budget analysis, needed to define for which AUV classes this position control system is effective from the perspective of energy consumption. Finally, Section VII draws some concluding remarks.

II. Application of the control station and ACK policy

To control the AUV trajectory the control station sends packets to the AUV containing the position coordinates in which the vehicle should head. Once the AUV receives a way-point, it starts moving toward the new position until either it reaches the destination or a new way-point is received. During a mission, the AUV sends monitoring packets to the control station containing information about its position and the direction it is moving towards. These packets are generated periodically. Moreover, the AUV acknowledges each received way-point, according to the following ACK policy. The AUV transmits the ACK piggybacked in a monitoring packet if a new packet is generated within a timeout to_{ACK} from the way-point reception. If no packets are generated within the timeout, the ACK is sent in a dedicated packet immediately after the timeout expires. All the packets containing an ACK are sent using a higher priority with respect to the other packets. In more detail, if the MAC of the node has some packets with a lower priority in its transmission queue, when a higher priority packet is received from the layer above it is transmitted first.[1]

The control station retransmits a way-point if the related ACK is not received until a timeout to_{retx}. The timeout is computed in an adaptive way as a function of the Round Trip Time (RTT)

$$to_{retx} = RTT + \alpha RTT \tag{1}$$

Each time a new way-point is transmitted by the control station the timeout is reset.

The designed mission combines detailed inspection of a small area (where the AUV has to move along several way-points close to each other) with large movements (where the AUV heads several kilometers far from the previous position). In the results we will notice that the retransmission policy is very effective to prevent errors in the long distance movements, while it is less effective in the case of small position changes, as when the packet should be retransmitted,

a new way-point has already been generated. More details on the path trajectory are presented in Section V.

III. Routing protocol for a multihop linear network

In a network composed by both nodes with a fixed and a mobile position, where the latter move towards different positions, the topology is not fixed, and therefore a static routing cannot be used. In this section we present two possible routing protocols that can be employed is such a network.

A. Flooding

Flooding is the easiest solution to forward a packet in a multihop network where the route is not static and the position of the receiver is unknown a priori. Flooding is considered to be robust in terms of packet delivery ratio, but is very energy inefficient and introduces a high risk of interference due to the large number of transmissions between all the nodes. However, the latter issue is mitigated in a linear network with only two nodes generating traffic (CTR and AUV) and the other nodes working as relays. Moreover, for each packet we set a flooding Time To Live (TTL) equal to the number of static nodes in the network. Flooding is our benchmark protocol, and in Section VI we present the performance of the multihop remote control system when employing such protocol.

B. Estimate-position based routing protocol (EPBR)

Estimate-position based routing (EPBR) is the new routing protocol we specifically designed for this paper in which the next hop is decided according to the estimated position of the AUV. In order to perform such estimate, the fixed nodes collect information about the position of the AUV and its direction of movement from the packets received from the other nodes. All the nodes deployed in this network need to know a priori the route to each node with a fixed position. This information can be either forwarded at network initialization by flooding, or directly stored in each node at network deployment. The number of relays is assumed to be constant throughout the network session, however, in case of position changes and/or node additions/failures, a new initialization has to be performed by employing the flooding protocol. Another assumption is that each node knows its own position as well. This is possible, as some commercial acoustic modems are equipped with a localization system within the device[2]. The protocol works differently for nodes with a fixed position (i.e., the relays and the control station) and for mobile nodes (such as AUVs).

EPBR for nodes with a fixed position behaves in two different ways, depending on the type of the destination node.

- When a node A with fixed position has to transmit a packet intended for another fixed node B, the protocol behaves like a static routing, where the route from A to B is set at the initialization.

---

[1]No preemption has been considered, as ongoing lower priority packet transmissions are not blocked when a higher priority packet reaches the MAC transmission queue.

[2]For instance the EvoLogics S2CR hydro-acoustic modem [**?**] can include a ultra-short baseline (USBL) acoustic positioning system.

- When a node A with fixed position has to transmit a packet intended for a mobile node V_1, it firstly estimates V_1's position.
    - If V_1 is in the transmission range of A, A forwards the packet directly to V_1.
    - Otherwise, A transmits the packet to the node C that A knows to be the closest to V_1 of all the nodes in A's transmission range.

EPBR for mobile nodes works differently, as the mobile node V_1 has just to transmit its packet to the closest node in its range.

The crucial part of this protocol is how to estimate the AUV position. In order to perform this operation, each node piggybacks in each packet the following information about each AUV in the network:

- the AUV position $P_1 = (p_{1x}, p_{1y}, p_{1z})$ sent by the AUV at instant t_1;
- the AUV next way-point $WP_1 = (w_{1x}, w_{1y}, w_{1z})$;
- the AUV speed $s_1 = (s_{1x}, s_{1y}, s_{1z})$;
- the time-stamp t_1 when the AUV was in position P_1.

Once a packet is received by a node A, such node checks if the time-stamp stored in the packet is more recent than its own time-stamp. If this is true, A updates its own information, otherwise A updates the information stored in the packet. Finally, to estimate the coordinates of the AUV position P_2^* at time t_2, A first performs the following operation

$$p_{2x}^* = p_{1x} + (t_2 - t_1) \cdot s_{1x} \cdot \sin \phi \cos \theta$$
$$p_{2y}^* = p_{1y} + (t_2 - t_1) \cdot s_{1y} \cdot \sin \phi \sin \theta \qquad (2)$$
$$p_{2z}^* = p_{1z} + (t_2 - t_1) \cdot s_{1z} \cdot \cos \phi \qquad ,$$

where

$$\theta = \arctan \frac{w_{1y} - p_{1y}}{w_{1x} - p_{1x}},$$
$$\phi = \arctan \frac{\sqrt{(w_{1x} - p_{1x})^2 + (w_{1y} - p_{1y})^2}}{w_{1z} - p_{1z}}, \qquad (3)$$

and then it checks whether P_2^* is between P_1 and WP_1. If this is true, the estimated position is P_2^*, otherwise the estimated position is WP_1, as the AUV has reached the way-point.

IV. MAC DESIGN FOR A MULTIHOP LINEAR NETWORK

In a multi-hop network, a Time Division Multiple Access (TDMA)-based MAC layer can be employed to exploit both pipeline and near-far effects [13]. The pipeline allows simultaneous transmissions from different nodes in the same time-slot, provided that the transmitting nodes are sufficiently separated in space not to interfere with each other. With the near-far effect, two adjacent nodes can transmit simultaneously as well. In this case, the high propagation delay of acoustic transmissions is exploited to avoid collisions. Consider two adjacent nodes A and B, transmitting to each other and starting the transmission of their own packet at the same time. If l is the packet length and r the bit rate, the time needed to transmit a packet is $t_{tx} = \frac{l}{r}$. If the propagation time between the two nodes is larger than the transmission time of a packet,

the signals will reach their destination nodes after these have finished their transmission, and therefore can be received and no deafness occurs. More in detail, if d is the distance between A and B and c is the sound speed, the near-far effect can be exploited if $\frac{l}{r} < \frac{d}{c}$. We consider various frame structures, from the simple TDMA to more advanced schemes using pipelining and near-far effects, showing how the frame length can be decreased in the latter cases. For illustration purposes, we consider here as an example the case with $N_{relays} = 3$ relay nodes, but provide a general expression for the length of the frame for the various cases.

1) The frame of the classical TDMA is reported in Table I, where the controller (CTR) is the first node transmitting, then the relays, in sequence from R_1 to R_4, and finally the AUV. In this way, a packet generated at the beginning of slot 1 takes $N_{relays}+1 = 4$ time slots to be forwarded from CTR to AUV, while a packet generated at the beginning of slot 5 needs at least $N_{relays}^2 + N_{relays} + 1 = 13$ time slots to be forwarded from AUV to CTR. This asymmetric link prioritizes the packet going from CTR to AUV, causing the packet sent from the AUV to be stored for a long time in the MAC queues of the relays. In order to have a symmetric link, the number of slots per frame allocated to each relay must be greater than or equal to the sum of the number of slots allocated to the nodes generating traffic (i.e., CTR and AUV). In our case, as both CTR and AUV can transmit for 1 time slot per frame, each relay must transmit for at least 2 time slots within a TDMA frame.

Slot number	1	2	3	4	5
Transmitting node	CTR	R_1	R_2	R_3	AUV

Table I
CLASSICAL TDMA CONFIGURATION WITH 3 RELAYS.

2) The frame of a fair solution (TDMA2way) without parallelism is presented in Table II, where CTR is the first node transmitting, then the relays, in sequence from R_1 to R_3, the AUV, and finally the relays again in reverse sequence from R_3 to R_1. In this way, in a frame of $2 \cdot (N_{relays} + 1) = 8$ time slots, a packet sent by CTR reaches AUV, and a packet sent by AUV reaches CTR.

Slot number	1	2	3	4	5	6	7	8
Transmitting node	CTR	R_1	R_2	R_3	AUV	R_3	R_2	R_1

Table II
TDMA2WAY CONFIGURATION WITH 3 RELAYS.

3) When two nodes are separated by 3 hops, they can transmit together without interfering with each other. This level of parallelism is called pipeline effect. The frame of the pipeline solution is presented in Table III, where CTR can transmit with R_3, and so can R_1 and AUV. In this way, in a frame of $2 \cdot N_{relays} + 1 = 7$ time slots, a packet sent by CTR reaches AUV, and a packet

sent by AUV reaches CTR. A more efficient pipeline

Slot number	1	2	3	4	5	6	7
Transmitting nodes	CTR R_3	R_1 AUV	R_2	R_3	R_3	R_2	R_1

Table III
TDMA PIPELINE CONFIGURATION WITH 3 RELAYS.

solution is presented in Table IV, where with 6 time slots the system is maintained stable. The latter solution is called TDMA efficient pipeline (TDMA-ep).

Slot number	1	2	3	4	5	6
Transmitting nodes	CTR R_3	R_1 AUV	R_2	R_3	R_2	R_1

Table IV
TDMA-EP CONFIGURATION WITH 3 RELAYS.

4) Two nodes can transmit together without interfering with each other when they are either separated by 3 hops (pipeline solution), or they are neighbor, but separated in space such that $\frac{l}{r} < \frac{d}{c}$, where r is the bit rate, l the length of the packet, d the distance between two nodes and c the propagation speed of acoustic waves. In this level of parallelism, we combine the pipeline effect with near-far effect. A possible configuration for the frame of the TDMA-nf solution is reported in Table V. In this way, in a frame of $2 \cdot N_{relays} = 6$ time slots, a packet sent by CTR reaches AUV, and a packet sent by AUV reaches CTR.

Slot number	1	2	3	4	5	6
Transmitting nodes	CTR R_1	R_1 AUV	R_2 R_3	R_2 R_3	R_2 R_3	R_1

Table V
CONFIGURATION OF TDMA-NF WITH 3 RELAYS.

The main advantage of TDMA-ep is that it lasts only 6 time slots for each value of $N_{relays} > 2$, thanks to the pipeline effect. Although TDMA-nf uses the slot parallelism more efficiently than all the other configurations, it is not effective in a network composed by mobile nodes, as simultaneous packets sent by adjacent nodes can interfere at a mobile receiver moving between them. For this reason, TDMA-nf will not be considered for our network simulations.

Also the configurations of TDMA-ep presented in this section are effective only for static networks. Indeed, transmissions by mobile nodes should not be parallelized, as their movement may cause changes in the topology. For this reason, TDMA-ep should include an additional time slot dedicated to each mobile node that patrols the network. Specifically, in a network composed by an AUV, TDMA-ep would employ 7 time slots. In Section VI, we compare the performance of TDMA2way with TDMA-ep for $N_{relays} = 4$. The best configuration of TDMA-ep is chosen using a brute force algorithm.

V. SIMULATION SCENARIO AND SYSTEM CONFIGURATION

The network topology considered for our simulations is reported in Figure 1. It is composed by a control station (CTR), four relays ($R_1 - R_4$) and one AUV. Both the control station and the relays are deployed from buoys to keep a fixed position, and are called static nodes, while the AUV patrols all the network area. The static nodes are spaced 3 Km from each other, thus the range in which the AUV can operate is extended to 12 Km from the base station. All the static nodes are placed 1 Km below the sea surface. The AUV operates 2.5 Km below the static nodes. The AUV trajectory is composed by both small and wide position changes. To drive the AUV during the inspection of a small area, with an average movement of 14.8 m, the way-points are sent every $t_{wp1} = 50$ s. To move the AUV to a different area 3 km apart, the way-points are sent every $t_{wp2} = 3150$ s. According to the way-points sent by the control station, the AUV should first patrol the area below the control station, then the area below each relay in sequence from R_1 to R_4, and finally it should come back to the control station, by inspecting again the area of each relay in reverse order. In the overall simulation, the AUV spends the same time below each relay. The path is described in Figure 2 (solid black line), where the initial point is $(-20, 60, -3500)$ and the final point $(-20, -60, -3500)$. The nodes communicate with each other using acoustic transmissions. The details of the simulation parameters are presented in Table VI.

Parameter	Value
Simulation length	40000 s
Acoustic source level	181 dB re 1μPa @ 1 m
Carrier frequency	25 kHz
Bandwidth	5 kHz
Data rate	4800 bps
AUV packet length	8000 bit
CTR packet length	2000 bit
to_{ACK}	10 s
α	1
AUV speed	1 m/s
Jammer source level	181 dB re 1μPa @ 1 m

Table VI
SIMULATION PARAMETERS.

The slot duration used in the TDMA has been computed to transmit exactly one packet for each slot in the worst case scenario, i.e., considering the maximum distance between two nodes and the maximum packet length. Therefore, the slot duration is equal to

$$t_{slot} = \frac{d_{MAX}}{c} + \frac{l_{MAX}}{r} + t_g \qquad (4)$$

where $d_{MAX} = 3000$ m is the maximum distance between two nodes, $l_{MAX} = 8000$ bit is the maximum packet length, $c = 1500$ m/s is the propagation speed of acoustic waves, r
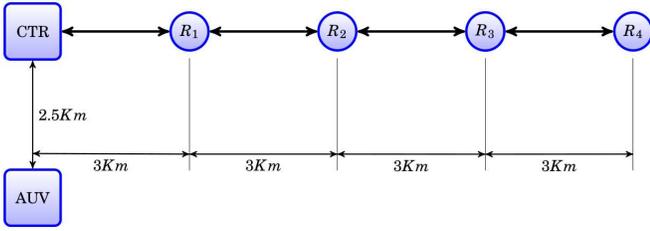
Figure 1. Network topology.

is the data rate, $t_g = 0.3$ s is a guard time used as safety margin. Moreover, we supposed that each node has a queue containing the packets to be transmitted at the MAC layer. In particular we consider a queue size equal to 2 packets for the AUV and equal to 100 packets for all the other nodes. When a queue is full, the new packets arriving from the upper layer are discarded. The TDMA configuration used to test both flooding and EPBR is listed in Table VII. As initial step, neither the pipeline nor the near-far technique has been exploited. Indeed, the main objective of this first analysis is to evaluate the feasibility of the remote control of the AUV, and for this reason a simple `TDMA2way` configuration has been employed. In the second analysis, we employed a more

Slot number	1	2	3	4	5	6	7	8	9	10
Transmitting node	CTR	R_1	R_2	R_3	R_4	AUV	R_4	R_3	R_2	R_1

Table VII
TDMA2WAY CONFIGURATION WITH N=4 RELAYS.

advanced MAC protocol that exploits both the near-far and the pipeline advantages. The frame configuration has been obtained with a brute force simulation, aimed to minimize the packet delivery delay, performed by imposing the constraints of the `TDMA-ep` protocol, presented in Section IV.

Slot number	1	2	3	4	5	6	7
Transmitting node	CTR R_3	R_1 R_4	R_2	AUV	R_2	R_1 R_4	R_3

Table VIII
TDMA-EP CONFIGURATION WITH N=4 RELAYS.

In Section VI we also report the behavior of the AUV using EPBR in a scenario with non negligible packet error rate. The system has been simulated using the DESERT Underwater Network Simulator [14].

VI. RESULTS AND PERFORMANCE COMPARISON

A. Routing and MAC performance

We report results for the remote control of the AUV path obtained with flooding and EPBR when employing the MAC presented in Table VII, by comparing the trajectory followed by the AUV with the path transmitted by the base station in the
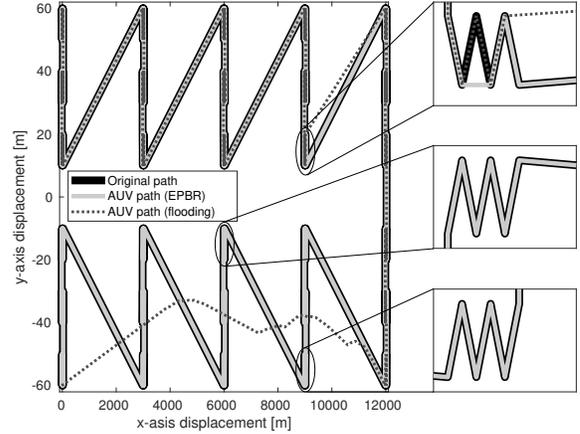

Figure 2. Path followed by the AUV using flooding, dotted gray line, and EPBR, solid gray line.
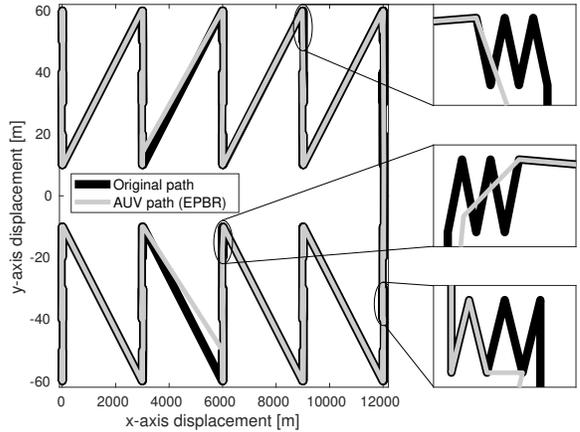

Figure 3. Path followed by the AUV using EPBR when the packet delivery ratio is equal to 0.69.

two cases. These results are depicted in Figure 2, where we can observe that the trajectory followed by the AUV significantly deflects from the original path (black line) when using flooding (dotted gray line). Differently, with EPBR (solid gray line), the AUV is able to follow the original path with high accuracy from the beginning to the end of the simulation. Indeed, the RMSE with flooding is 3447 m and with EPBR is 5.5 m. These results have been obtained when the AUV generates a packet every 30 s.

EPBR has also been tested with a non-negligible packet loss to check the robustness of the protocol in critical situations. Two nodes have been used as jammers to simulate a non-negligible packet error rate. The nodes have been placed in the network between relays R_1 and R_2 and between relays R_3 and R_4. These nodes generate packets according to a Poisson process, independently from each other. The average jamming packet period has been set to 50 s. The jammers transmit in the same band as the other nodes in the network. Figure 3
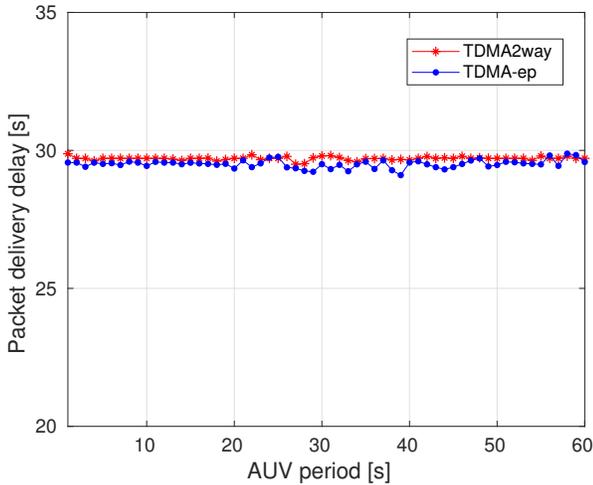
Figure 4. Average packet delivery delay of way-points.

Figure 5. Average packet delivery delay of packets generated by the AUV.

Figure 6. Average throughput received by the control station.

reports the path followed by the AUV (solid gray line) in a scenario with a packet delivery ratio equal to 0.69, calculated as the ratio between the number of packets received and the number of packets transmitted during the entire simulation. In the zoomed part we can observe a deviation from the original path (solid black line) due to the loss of some way-points. However, we can highlight that the AUV never gets stuck or loses completely the original trajectory.

After testing the feasibility and the robustness to packet losses of the EPBR protocol, in the second step we employed the TDMA-ep scheme reported in Table VIII to improve the performance in terms of packet delivery delay and throughput. We compared the results obtained using TDMA-ep with those obtained employing TDMA2way reported in Table VII. The average packet delivery delay for way-points is depicted in Figure 4. The delay has been computed for different values of the AUV period, i.e., the time between the generation of two AUV packets, ranging from 1 to 60 s. The obtained control packet delivery delay is very similar for the 2 MAC configurations, and is independent of the generation period of the AUV packets, confirming the effective design of both MAC protocols. The average packet delivery delay for the packets generated by the AUV is reported in Figure 5, when considering different values of the AUV period.

The network is kept stable as long as the AUV period is bigger than the frame duration of both TDMA-ep and TDMA2way. On the other hand, for AUV period smaller than the frame duration the packet delivery delay increases linearly when decreasing the AUV period. This is because the MAC frames are designed to make the AUV transmit only one packet during an entire time frame. Therefore, if more than one packets per frame are generated, the exceeding ones are stored in the AUV queue at the MAC layer, causing an increase of the packet delivery delay. When the AUV period is smaller than the frame duration (27.77 s for TDMA-ep and 39.67 s for TD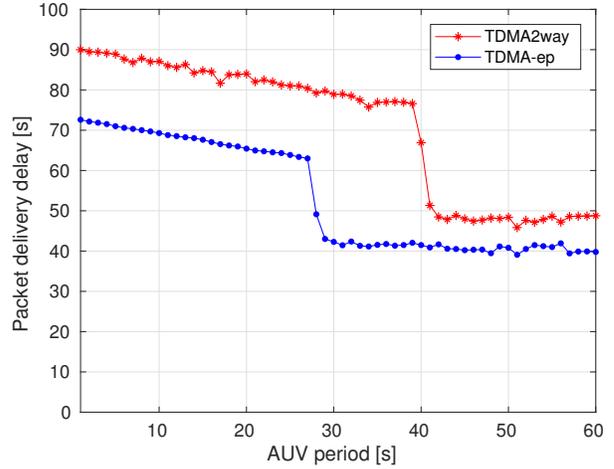MA2way) the network becomes unstable and packets are accumulated in the queue of the AUV. This results in the almost-vertical slope of the packet delivery delay in Figure 5, for values of the AUV period around the frame length of the TDMA schemes. If the AUV period decreases even further, the delay correspondingly increases, approaching the asymptotic value for infinite traffic. Since TDMA-ep has a smaller frame duration than TDMA2way, it supports a higher AUV traffic generation, providing a shorter packet delivery delay.
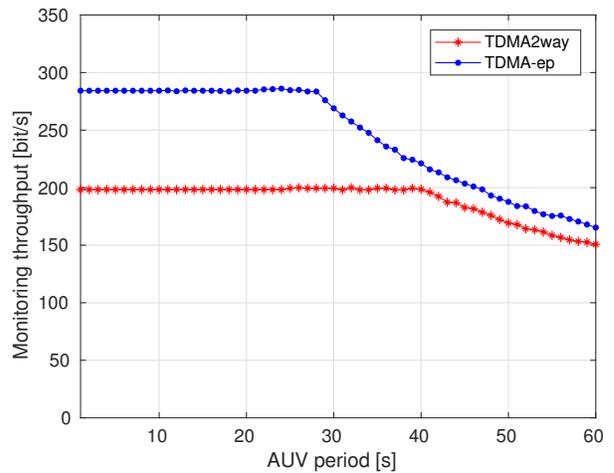
Figure 6 reports the throughput received by the control station. Also in this case, TDMA-ep outperforms TDMA2way. The frame duration of TDMA-ep is 27.77 s, that is 11.90 s smaller than in TDMA2way (that has a frame duration of 39.67 s), therefore TDMA-ep supports a smaller generation period and provides a higher throughput. For an AUV period smaller than the frame duration the throughput remains constant, since only one packet per frame is actually transmitted.

B. Power budget

We analyzed the energy consumption of the AUV during its mission. The power consumptions of the AUV and of the modems are obtained from the data-sheets of products available off-the-shelf. In particular, we supposed to use the EvoLogics S2CR 18/34 hydroacoustic modem with a power consumption of $P_{modem} = 80$ W [15] and a Folaga AUV equipped with a battery of 1.25 kWh [16]. According to the data-sheets, the Folaga can perform a mission of 14 hours at a speed of 1 m/s. The duration does not consider the energy consumed by the modem for the transmission of packets. From this data, we can infer the power consumption of the AUV with

$$P_{AUV} = \frac{\text{battery energy}}{\text{max duration}} = \frac{1250}{14} = 89.3 \text{ W.} \qquad (5)$$

Considering the length of the mission $t_{mission} = 11.11$ hours, the energy consumption of the vehicle is equal to

$$E_{AUV} = P_{AUV} \cdot t_{mission} = 992.12 \text{ Wh.} \qquad (6)$$

To evaluate the feasibility of the mission, we also include the energy consumption of the modem. We consider the worst case scenario, with the AUV generating the maximum packet load supported by the network, i.e., transmitting an AUV packet per frame using `TDMA-ep`. In this scenario the modem transmits $N_p = 1438$ packets during the full mission. Since to transmit a packet the modem employs

$$t_{tx} = \frac{\text{packet length}}{\text{data rate}} = \frac{8000}{4800} = 1.67 \text{ s,} \qquad (7)$$

the overall amount of time a modem is occupied to transmit is

$$t_{tx_{AUV}} = N_p \cdot t_{tx} = 2401.46 \text{ s,} \qquad (8)$$

and the energy consumption of the modem is

$$E_{tx} = P_{AUV} \cdot t_{tx_{AUV}} = 53.6 \text{ Wh.} \qquad (9)$$

Therefore, the overall energy consumption of the AUV is $E = E_{AUV} + E_{tx} = 1045.72$ Wh, smaller than the energy of the battery equipped in the AUV Folaga. Therefore, from an energy point of view, such mission might be performed by a Folaga AUV and the transmission of packets accounts for only 5.13% of the overall consumption.

Considering bigger AUVs, such as A9-E equipped with a battery of 4.2 kWh [17], or Hugin 4500 with a battery of 24 kWh [18], the impact of the packet transmissions on the overall energy consumption becomes negligible, i.e., 2.5% and 0.7%, respectively.

VII. Conclusions

We presented a feasibility study of the control of an AUV trajectory via an underwater multi-hop linear network, where both pipeline and near-far effects have been exploited by the MAC to maximize the network performance. In addition, we designed the Estimate-Position Based Routing networking protocol, used to change the packet routes according to the estimated position of the submerged vehicle. This network has been simulated and analyzed using the DESERT underwater network simulator, in both ideal scenarios and in the presence of acoustic jammers. Through this study, we provided an idea of the possible Quality of Service that such system can provide in terms of both control accuracy and monitoring traffic. Further work will focus on an adaptive MAC layer, where the slot assignment changes according to the maximum number of hops needed to forward the packet between the base station and the AUV.

References

[1] J. Proakis, E. Sozer, J. Rice, and M. Stojanovic, "Shallow water acoustic networks," *IEEE Communications Magazine*, vol. 39, no. 11, pp. 114–119, Nov. 2001.

[2] R. W. Coutinho, A. Boukerche, L. F. Vieira, and A. A. Loureiro, "Geographic and opportunistic routing for underwater sensor networks," *IEEE Transactions on Computers*, vol. 65, no. 2, pp. 548–561, Feb. 2016.

[3] J. Heidemann, M. Stojanovic, and M. Zorzi, "Underwater sensor networks: applications, advances and challenges," *Philosophical Transactions of the Royal Society A*, vol. 370, no. 1958, pp. 158–175, Jan. 2012.

[4] A. Micallef, S. Krastel, and A. Savini, *Submarine Geomorphology*. Springer, 2017.

[5] "Wireless For Subsea Seatooth," accessed: March. 2018. [Online]. Available: http://www.wfs-tech.com/index.php/products/seatooth/

[6] M. Doniec, M. Angermann, and D. Rus, "An End-to-End Signal Strength Model for Underwater Optical Communications," *IEEE Journal of Oceanic Engineering*, vol. 38, no. 4, pp. 743–757, Oct. 2013.

[7] F. Campagnaro, F. Favaro, P. Casari, and M. Zorzi, "On the Feasibility of Fully Wireless Remote Control for Underwater Vehicles," in *Proc. Asilomar Conf. SS&C*, Pacific Grove, CA, Nov 2014.

[8] F. Campagnaro *et al.*, "Multimodal underwater networks: Recent advances and a look ahead," in *Proc. ACM WUWNet*, Halifax, Canada, Nov. 2017.

[9] R. B. Wynn, V. A. Huvenne, T. P. Le Bas, B. J. Murton, D. P. Connelly, B. J. Bett, H. A. Ruhl, K. J. Morris, J. Peakall, D. R. Parsons *et al.*, "Autonomous Underwater Vehicles (AUVs): Their past, present and future contributions to the advancement of marine geoscience," *Marine Geology*, vol. 352, pp. 451–468, Jun. 2014.

[10] "Scout USBL Underwater Tracking System," accessed: March 2018. [Online]. Available: https://www.sonardyne.com/product/scout-usbl-underwater-tracking-system/

[11] "Fusion 6G Long Baseline Positioning (LBL) System," accessed: March 2018. [Online]. Available: https://www.sonardyne.com/product/fusion-6g-long-baseline-positioning-lbl/

[12] F. Campagnaro, F. Guerra, F. Favaro, V. S. Calzado, P. Forero, M. Zorzi, and P. Casari, "Simulation of a multimodal wireless remote control system for underwater vehicles," in *Proceedings of the 10th International Conference on Underwater Networks & Systems (WUWNet)*. ACM, 2015, p. 32.

[13] P. Anjangi and M. Chitre, "Design and implementation of super-tdma: A mac protocol exploiting large propagation delays for underwater acoustic networks," in *Proceedings of the 10th International Conference on Underwater Networks & Systems (WUWNet)*. ACM, 2015, p. 1.

[14] R. Masiero, S. Azad, F. Favaro, M. Petrani, G. Toso, F. Guerra, P. Casari, and M. Zorzi, "DESERT Underwater: An NS-Miracle-based framework to design, simulate, emulate and realize test-beds for underwater network protocols," in *Proc. MTS/IEEE Oceans*, Yeusu, Korea, May 2012.

[15] EvoLogics, "Data sheet modem EvoLogics S2CR 18/34," https://www.evologics.de/files/DataSheets/EvoLogics_S2CR_1834D_Product_Information.pdf, [Online]; accessed March 2018.

[16] Graal Tech, "Folaga data sheet," https://www.graaltech.com/folaga-features, [Online]; accessed March 2018.

[17] ECA Group, "A9-e data sheet," http://eca-media.ecagroup.com/player/pdf?key=c76073dba4f3a6cc6a81f47b55c4e96a, [Online]; accessed March 2018.

[18] Kongsberg, "The hugin family," https://www.km.kongsberg.com/ks/web/nokbg0397.nsf/AllWeb/A6A2CC361D3B9653C1256D71003E97D5/$file/HUGIN_Family_brochure_r2_lr.pdf?OpenElement, [Online]; accessed March 2018.